Uncertainty in mechanical deformation of a Fabry-Perot cavity due to pressure: towards best mechanical configuration

S. Moltó[1], M. A. Sáenz-Nuño[2], E. Bernabeu[3], M. N. Medina[1]

[1] *Centro Español de Metrología, Calle Alfar 2, 28760 Tres Cantos, España*
[2] *Instituto de Investigación Tecnológica, Escuela Técnica Superior de Ingeniería-ICAI, Universidad Pontificia Comillas, 28015 Madrid, España*
[3] *Universidad Complutense de Madrid, España*

ABSTRACT
In this paper, a study of the deformation of a refractometer use to achieve a quantum realization of the Pascal is made. First, the propagation of the uncertainty in the measure of pressure due to mechanical deformation was made. Then deformation simulations were made with a cavity designed by the CNAM and whose results are reported in the 18SIB04 Quantumpascal EMPIR project. This step aims to corroborate the methodology used in the simulations. The pressure-normalized relative deformation of this design obtained in 18SIB04 is (-6.390 ± 0.015) × 10^{-12} Pa^{-1}, the result obtained with our method is (-6.384 ± 0.032) × 10^{-12} Pa^{-1}, which differs 0.001 times from the value obtained in 18SIB04. Finally, a cylindrical cavity design is presented and simulated obtaining a pressure-normalized relative deformation of (-5.758584 ± 0.00000047) × 10^{-12} Pa^{-1}, which deforms 0.1 times less.

Corresponding author: S. Moltó, e-mail: smolto@cem.es

1. INTRODUCTION

The 18SIB04 QuantumPascal EMPIR project deals with the development of a quantum-based pressure standard in order to improve the uncertainty and traceability that the current methods offer. This project is based on the application of a Fabry-Perot interferometer to measure in a pressure range of 1 Pa to 100 kPa. However, some parameters must be carefully handled, such as the deformation, the temperature and the gas properties.

The cavity deformation due to the gas pressure was simulated using a finite element method (FEM) software. Therefore, a study of the uncertainty obtained in these simulations and its propagation in the evaluation of pressure was needed.

A previous study of the simulated cavity deformation due to pressure was carried out in [1], and its results were used herein to show the difference obtained due to the use of different software. Finally, a new cylindrical design of the cavity was proposed and compared to the design proposed in [1].

2. THEORY

The relative deformation in the length with the gas pressure of the Fabry-Perot cavity can be described with a linear dependency as in equation (1). Where L_0 is the without deformation cavity length, ΔL is the change in cavity length (the deformation), P is the pressure and κ is the pressure-normalized deformation.

$$\frac{\Delta L}{L_0} = \kappa P \, . \tag{1}$$

L_0 is calculated as the distance between the centre of the reflective face of the mirrors, and ΔL as the change in this distance.

Table 1 summarizes the data used in this work, so is it possible to calculate the pressure with equations below with the values of the table.

Table 1. Coefficients and constants used in this work

Parameter	Designation	Value
L_0	Cavity length in vacuum	0.1 m
n	Refractive index	$n \geq 1$
A_r	Molecular polarizability	$4.44613930 \times 10^{-6}$ m³/mol [2]
B_r	First refractive virial coefficient	0.812×10^{-12} m⁶/mol² [2]
$\widetilde{B_\rho}$	First density virial coefficient	$-[1 + 4(B_r/A_r^2)]/6$ [2]
$B_P(T)$	First pressure virial coefficient	$[-4.571 + 0.1974(T(K) - 300) - 5.137 \times 10^{-4}(T(K) - 300)^2] \times 10^{-6}$ m³/mol [2]
ξ	Mirror dispersion coefficient	11×10^{-6} [2]
η	Gas dispersion coefficient	1×10^{-6} [2]
λ_0	Wavelength in vacuum	632.8 nm
λ	Wavelength affected by pressure	$\lambda = \lambda_0/n$
ν_0	Frequency in vacuum	c/λ_0
q_0	Number of length modes in vacuum	$2L_0/\lambda_0$
$\Delta\nu$	Laser change in frequency	Assumed as 0
Δq	Change in number of modes	Estimate in Equation (4)
ϵ	Deformation coefficient	Equation (3) [3]
T	Temperature	273 K
P	Nominal Pressure	From 1Pa to 10 kPa
N_A	Avogadro number	Used value of [3]
k_B	Boltzmann constant	Used value of [3]

The gas parameters can be calculated from the refractivity, whose change is related to the change of the laser frequency $\Delta\nu$, the change in the number of modes (Δq) and the deformation coefficient (ϵ) using equation (2), [3]. This equation can be used with absolute pressures up to 10 kPa.

$$\Delta(n-1) = (n-1) = \frac{\frac{\Delta q}{q_0} + (1 + 2\xi + \eta)\frac{\Delta\nu}{\nu_0}}{1 + \epsilon + (1 + 2\xi + \eta)\frac{\Delta\nu}{\nu_0}}. \quad (2)$$

The deformation coefficient (ϵ) [3] depends on the pressure-normalized deformation (κ) as it is shown in equation (3). The change in number of modes is an experimental measurement but it can be simulated using equation (4), where λ_0 is the wavelength in vacuum and λ is the wavelength affected by the change in refractive index ($\lambda = \lambda_0/n$). Also, $\Delta\nu$ is the laser change in frequency which maximum value is ν_{FSR} when mode jumping is used.

$$\epsilon = \frac{\kappa P}{(n-1)} = \kappa \frac{2 k_B T N_A}{3 A_r} \quad (3)$$

$$\Delta q = q - q_0 = \frac{L}{\frac{\lambda}{2}} - \frac{L_0}{\frac{\lambda_0}{2}} = 2L_0 \left[\frac{\lambda_0 + \lambda_0 \kappa P - \lambda}{\lambda \lambda_0}\right]. \quad (4)$$

The molar density is related with the refractivity by the equation (5) [3] and the molar density is related with the pressure by the equation (6) [3]. Where B_ρ is the first virial coefficient and $B_P(T)$ is the first pressure virial coefficient which is calculated with $[-4.571 + 0.1974(T(K) - 300) - 5.137 \times 10^{-4}(T(K) - 300)^2] \times 10^{-6}$ m³/mol.

$$\rho = \frac{2}{3 A_r}(n-1)[1 + \widetilde{B_\rho}(n-1)] \quad (5)$$

$$P = k_B T N_A \rho[1 + B_P(T)\rho]. \quad (6)$$

3. UNCERTAINTY PROPAGATION

In order to calculate the uncertainty of pressure due to the uncertainty in κ is necessary to obtain an expression of pressure depending on κ directly. From equations (5), (6) and the expression of $B_P(T)$ is possible to calculate that relation (equation (7)), where the value of C_0 is shown in equation (8)

$$P(\Delta\nu, \Delta q, \kappa, T) = $$
$$\frac{C_0 T \Delta q}{(C_0 T \kappa + 1)q_0}\left(\frac{B_\rho \Delta q}{(C_0 T \kappa + 1)q_0} + 1\right)$$
$$\times \left(1 + \frac{2 \Delta q\left(\frac{B_\rho \Delta q}{(C_0 T \kappa + 1)q_0} + 1\right)}{3 A_r(C_0 T\kappa + 1)q_0}B_P(T)\right) \quad (7)$$

$$C_0 = \frac{2 N_A k_B}{3 A_r}. \quad (8)$$

Considering that $\Delta q = \frac{2L_0(1 + \kappa P_{\text{Nominal}})}{\lambda/2} - q_0$ and $\Delta\nu = 0$ an expression of pressure as $P = P(\kappa, P_{\text{Nominal}}, T)$ is obtained (Equation (9))

$$P(\kappa, P_{\text{Nominal}}, T) = $$
$$\frac{C_0 T \left(\frac{2(L_0 P_{\text{Nominal}} \kappa + L_0)}{\lambda} - q_0\right)}{(C_0 T \kappa + 1)q_0} \times $$
$$\left(\frac{B_\rho \left(\frac{2(L_0 P_{\text{Nominal}} \kappa + L_0)}{\lambda} - q_0\right)}{(C_0 T \kappa + 1)q_0} + 1\right) \times \quad (9)$$

$$\left(\frac{2B_P \left(\frac{2(L_0\, P_{\text{Nominal}}\, \kappa + L_0)}{\lambda} + q_0 \right)}{3\, A_{\mathrm{r}}(C_0\, T\, \kappa + 1) q_0} \times \right.$$
$$\left. \left(\frac{\frac{2(L_0\, P_{\text{Nominal}}\, \kappa + L_0)}{\lambda} - q_0}{(C_0\, T\, \kappa + 1) q_0} + 1 \right) + 1 \right).$$

In this work, it is assumed that the only source of uncertainty is the pressure-normalized deformation (κ), as the aim is to analyse how this particular magnitude affects to the measurement of pressure. From equation (7) and applying the rule of the propagation of uncertainty the equation (10) is obtained, which estimates the relative uncertainty in pressure with respect κ. Where C_κ is the sensitivity coefficient, which is calculated with equation (11). As the pressure of equation (9), depends on the nominal pressure, the relative uncertainty depends on that parameter

$$w(P) = \frac{u(P)}{P} \approx \left| C_\kappa \frac{u(\kappa)}{\kappa} \right| \tag{10}$$

$$C_\kappa = \frac{\partial P(\kappa, P_{\text{Nomina}}, T)}{\partial \kappa}. \tag{11}$$

4. CNAM CAVITY DESCRIPTION

The cavity modelled for the simulation was built by the CNAM ([5]). In Figure 1, it is shown a 3D model of the Fabry-Perot cavity. The spacer is made of Zerodur and the mirrors are made of fused silica. The dimensions of the Zerodur spacer are specified in Figure 2. The mirrors were considered to be flat.

The properties of the materials used are collected in Table 2. In order to improve the computational time, only an octave of the cavity was simulated using the symmetry restrictions available in the software. This selection is represented in Figure 3 where the simulated section of the Fabry-Perot cavity is dyed with red.

With the purpose of simulating the cavity inside a vacuum chamber, the same pressure load was introduced to every face of the Fabry-Perot cavity (same inner and outer pressure). The only

Table 2. Materials properties used in the simulations.

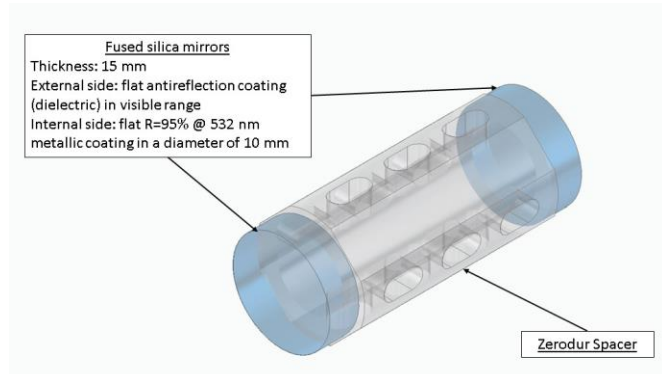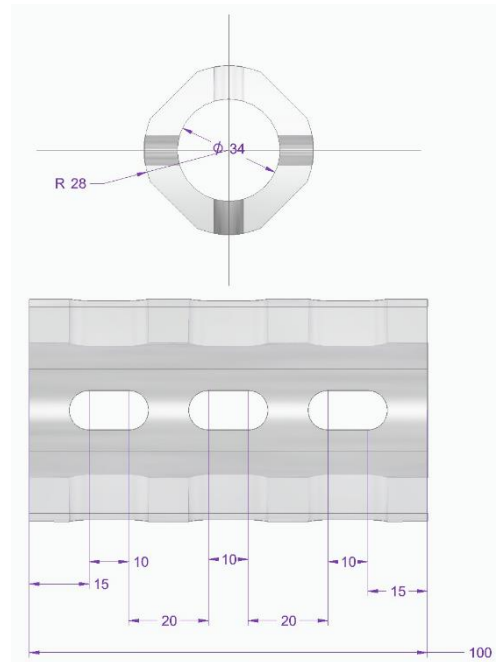| Parameter	Spacer material (Zerodur)	Mirror material (fused silica)
Young modulus (GPa)	90.3	73
Poisson ratio	0.24	0.155
Density (kg/m³)	2530	2195

Figure 1. FP cavity model.

Figure 2. Dimensions of the Zerodur spacer in mm, all drillings diameters are 10 mm.
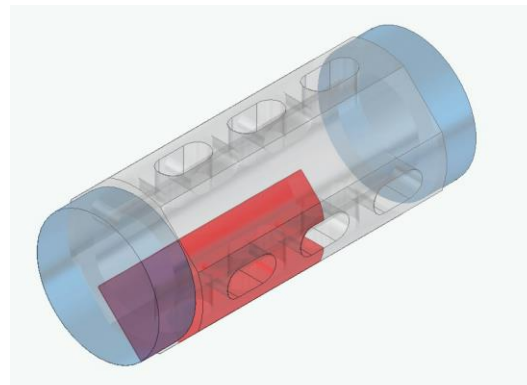

Figure 3. CNAM FP cavity model with the simulated section dye in red.

restriction applied to the model was that the spacer and the mirrors would not rotate.

5. SIMULATION RESULTS

The Solid Edge 2021 results are shown with a colormap of the deformation in mm in Figure 4. It was shown an inhomogeneous deformation, but it was corrected using the symmetries of the design. Simulating a part of the model incorporates these symmetries without including extra conditions to the model.

5.1. Cavity Relative Deformation Dependency with the Number of Mesh Elements.

The relative deformation of the cavity calculated in the simulation depends on the number of mesh elements used, as it is shown in Figure 5. The convergence of κ with the number of mesh elements was not achieved so two curve fits were made. One to the function $y_1(x) = a\, x^{-4} + b\, x^{-2} + c\, x^{-1} + d$ and another to $y_2(x) = a\, (\log(b\, x))^{-1} + d$, where x is the number of mesh elements and y_i is the value of κ. These functions where selected to be constant when the number of mesh elements from
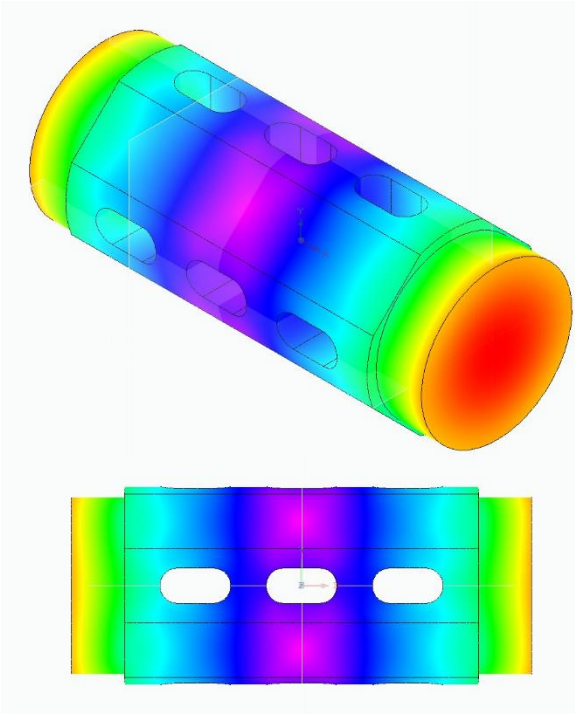
Figure 4. Cavity deformation for a pressure of 80 kPa.

Table 3. Values of the mean square error (MSE) of the fit, the mean absolute error (MAE) of the fit and κ in Pa^{-1} for each fit.

$y_1(x) = ax^{-4} + bx^{-2} + cx^{-1} + d$		
MSE	MAE	
1.41×10^{-23}	2.83×10^{-12}	
κ	u(κ)	u(κ)/κ
-6.38378×10^{-12}	3.2×10^{-16}	4.9×10^{-5}
$y_2(x) = a(\log(bx))^{-1} + d$		
MSE	MAE	
4.78×10^{-31}	4.85×10^{-16}	
κ	u(κ)	u(κ)/ κ
6.3868×10^{-12}	1.7×10^{-15}	2.7×10^{-4}

that near 0 Pa there is an asymptotic behaviour, but if the nominal pressure increases a linear dependency is presented.

As it was said before, the relative uncertainty of pressure depends on the nominal pressure (equation (10) and (11)). Figure 7 represents the evolution of pressure uncertainty with the nominal pressure. It is shown a linear dependency and the uncertainty obtained by using κ_2 increases faster than the one obtained with κ_1. Also, the relative uncertainty in pressure calculated in a range of pressure under 10 kPa is under 9×10^{-12}.

5.2. Comparison with Results from [1]

A comparison between the results of simulations made with different software and institution are needed to verify that the procedure of simulation of every participant in the 18SIB04 QuantumPascal EMPIR project is correct.

In [1] the results of simulating the deformation of the Fabry-Perot cavity are shown, and they are collected in Table 4. The result simulated in Solid Edge software by the CEM is less than 10^{-3} time bigger than the average of [1]. The uncertainty in CEM's simulation was calculated as a rectangular distribution centred in -6.3846×10^{-12} Pa^{-1} and with a width equal to two times the

among group of functions that tends to infinite as it is shown in equation (12):

$$\lim_{x \to \infty}(a\,x^{-4} + b\,x^{-2} + c\,x^{-1} + d) = d = \kappa$$
$$\lim_{x \to \infty}\left(\frac{a}{\log(b\,x)} + d\right) = d = \kappa. \tag{12}$$

The values obtained in the fitting are collected in Table 3. Using equation (12) it is obtained the value of κ for each curve fit. The value for y_1 is $\kappa_1 = (-6.38378 \times 10^{-12} \pm 3.2\ 10^{-16})$ Pa^{-1} and for y_2 is $\kappa_2 = (-6.3868 \times 10^{-12} \pm 3.2\ 10^{-15})$ Pa^{-1}. The uncertainty is calculated with the variance and covariance matrix obtained with function *curve_fit()* from the package optimize of Scipy [3], that uses the equation $\mathrm{cov}(x,y) = C_{xy} = \frac{1}{N}\sum_i(x_i - \bar{x})(y_i - \bar{y})$ to estimate it. It is shown that the first curve gives less uncertainty than the second.

With the relative deformation of the cavity over the pressure obtained in Table 3, the values of Table 1 and the equation (9) is possible to calculate the pressure that the Fabry-Perot cavity will have for a given nominal pressure, obtaining in Figure 6 the difference between the calculated and nominal values. It is shown
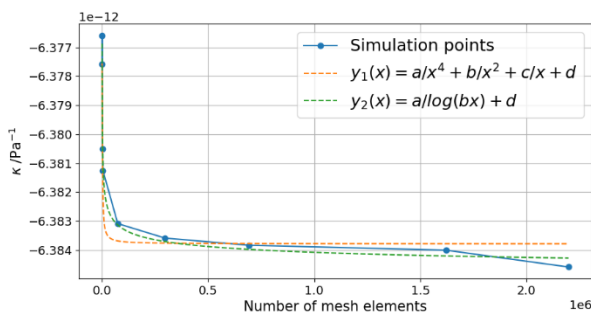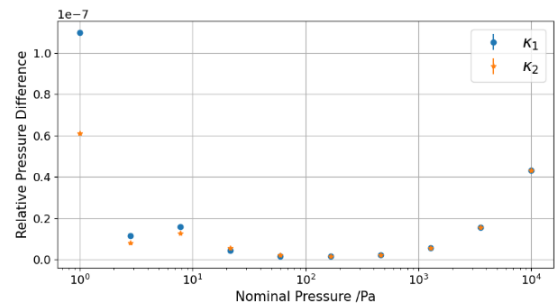

Figure 6. Relative difference between calculated pressure and nominal pressure ((P_{Nominal}-P)/P_{Nominal}), where κ_1 is the value of pressure-normalized deformation calculated with y_1 and κ_2 is the value of pressure-normalized deformation calculated with y_2.
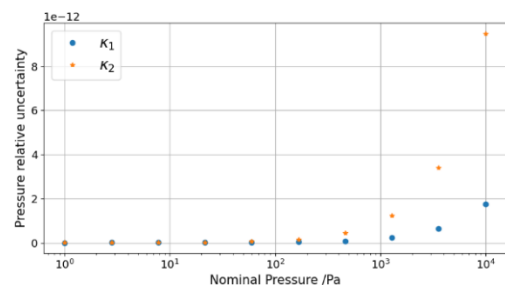

Figure 5. Pressure-normalized deformation versus number of mesh elements. The data was fitted to two curves

Figure 7. Relative uncertainty of calculated pressure with κ_1 = -6.38378 Pa^{-1} and κ_2 = 6.3868 Pa^{-1} versus the nominal pressure.

Table 4. Summary of the simulated pressure normalized cavity deformation using the finest meshing by each partner and software.

Partner - Software Used	Pressure-normalized deformation (κ) $\Delta L/L/P$ in 10^{-12} Pa^{-1}	Number of mesh elements
A-Comsol [1]	-6.3900	1 735 324
B-Comsol [1]	-6.3899	190 000
B-Ansys [1]	-6.3908	2 948 108
C-Ansys [1]	-6.3900	21 061
D-Comsol [1]	-6.3902	3 168 777
Average value [1]	-6.3902	--
Standard error of the mean (σ_x) [1]	0.00015	--
CEM-Solid Edge	-6.3846	2197477
Uncertainty	0.0032	--

difference of CEM's value and the average value of [1] (2.24×10^{-14} Pa^{-1}).

Using the values of Table 4, Table 1 and equation (7), the value of pressure for the average value κ and the value calculated with Solid Edge are obtained. In Figure 8 the relative difference of each pressure with respect the nominal pressure is represented. It is shown the same behaviour as in Figure 6. Also, the values are so similar that the effect on the pressure cannot be distinguished with this figure for pressures over 10 Pa; hence, in Figure 9, the relative difference of the pressure calculated with the κ obtained by [1] and the pressure calculated with κ obtained with Solid Edge is represented.

In Figure 9, the same asymptotic behaviour is shown. The maximum relative difference obtained is near 0 Pa, where the asymptote is located, is around 3.5×10^{-8}. After the elbow value of the function the relative difference in pressure is less than 2×10^{-10}.
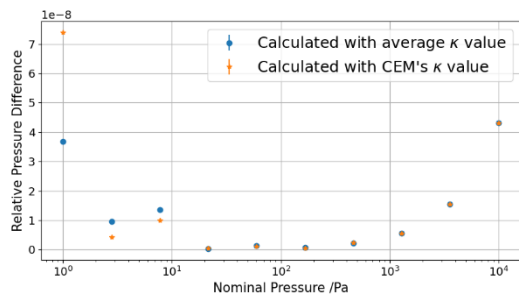

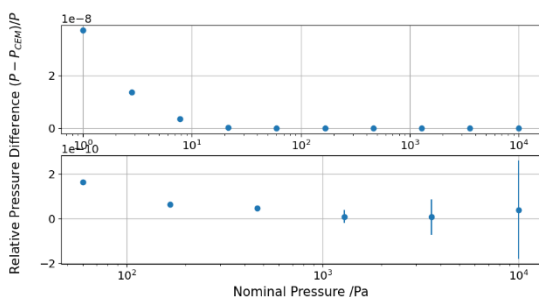Figure 8. Relative difference between calculated pressure and nominal pressure (($P_{Nominal}$–P)/$P_{Nominal}$).

Figure 9. Relative difference between calculated pressure and nominal pressure ((P-P_{CEM})/P), where P is the nominal pressure and P_{CEM} is the calculated pressure. In the first figure the uncertainty is not appreciable, but in the enlargement below the uncertainty can be seen.
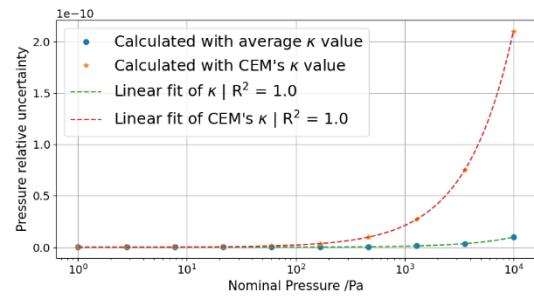

Figure 10. Relative uncertainty of calculated pressure with κ obtained by [1] and κ calculated by the CEM with Solid Edge software versus the nominal pressure. R^2 is the linear correlation coefficient.

As the relative uncertainty of pressure depends on the nominal pressure (Equation (10) and (11)), Figure 10 depicts the evolution of pressure uncertainty with the nominal pressure. It is shown a lineal dependency and the uncertainty of the pressure obtained with the CEM's value increase faster. Also, the relative uncertainty calculated for the range of pressure where equation (2) is acceptable is under 3×10^{-10}.

6. CEM'S CYLINDRICAL CAVITY

With the purpose of solving the symmetry rupture that supposes using the spacer as an inner vacuum chamber and gases chamber, a new cylindrical design was proposed.

6.1. Cavity Description

The designed cavity is represented in Figure 11, where the simulated section is coloured in red. Although this time the symmetry is only a quarter of the model and not an octave as before, an octave was taken after checking that the results were the same as the full model. This way, a similar number of mesh elements are analysed for both models. The spacer and mirrors of this cavity are made of Schott's Zerodur Class 0, whose properties are shown in Table 2. The Zerodur Class 0 mirrors provide a reflectance over 97 % for a wavelength of 633 nm, which is the wavelength that will be used in the pattern.

The dimensions of the Zerodur spacer are specified in Figure 12. It is shown that the geometry of this spacer is simpler than the presented in Figure 2, this will deal with faster calculations.

The inner diameter of the Zerodur spacer was selected to be 20 mm, so as to be compatible with the optic requirements of numeric aperture of 0.2. Also, this diameter provides a more

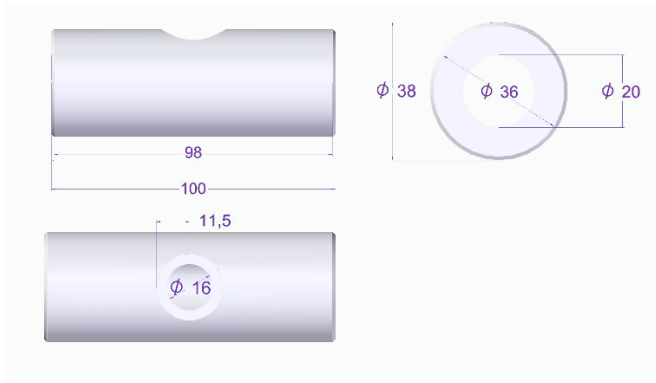Figure 11. CEM FP cavity model with the simulated section dyed in red.

Figure 12. Dimensions of the Zerodur spacer in mm.

laminar regimen in rapid pressure variations than with smaller diameters. The Zerodur spacer thickness was designed to be 9 mm, but the mirror thickness was 11 mm, which corresponds to a relative factor $\frac{Mirror\ Thickness}{Spacer\ Thickness} \approx 1.22$, similar to the Bessel's function first zero divided by π $\left(\frac{J_1(z)}{\pi} = 1.216\right)$. The Bessel function is associate to the circular revolution of 2π of the cylindrical symmetry.

As made with the previous cavity, in order to simulate that the cavity is into a vacuum chamber, the same pressure load was introduced to every face of the Fabry-Perot cavity. The only restriction applied to the model was that the spacer and the mirrors would not rotate.

6.2. Results of the simulations

Figure 13 presents the results of the deformation simulation for a pressure of 80 kPa. As shown in Figure 4, there was an inhomogeneous deformation, but it is corrected by using the partial simulation of the model as the partial only simulates one mirror assuming the symmetry.

The simulation data were fitted to three different equations. There were selected to be constant when the number of mesh elements tends to infinite. The selected curves are shown in
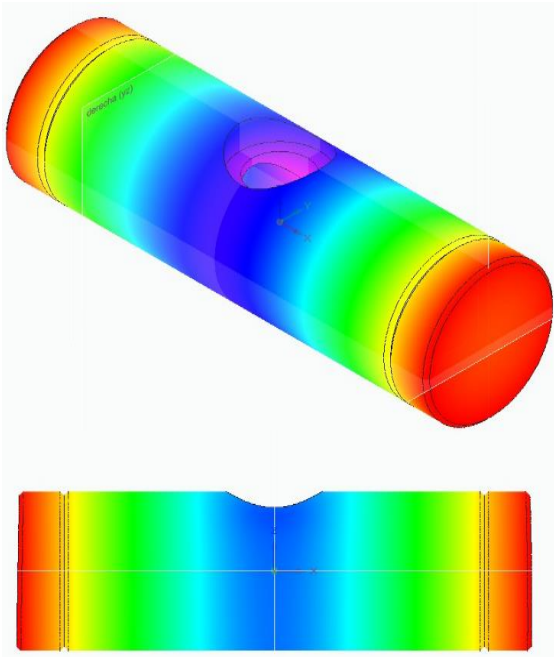

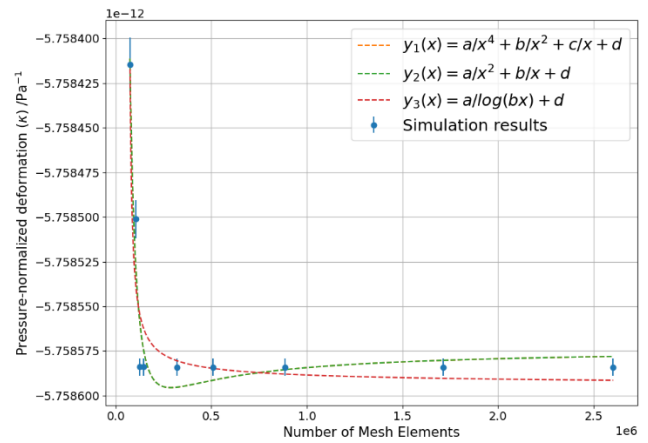Figure 13. Cylindrical cavity deformation for a pressure of 80 kPa.

Figure 14. Pressure-normalized deformation versus the number of mesh elements. The data were fitted to three equations.

equation (13), the quadratic equation was not added in equation (12) because the software could not fit the data to that curve. The results of fitting are shown in Figure 14, where the curves $y_1(x)$ and $y_2(x)$ cannot be distinguish.

$$y_1(x) = a\,x^{-4} + b\,x^{-2} + c\,x^{-1} + d$$
$$y_2(x) = a\,x^{-2} + b\,x^{-1} + d \tag{13}$$
$$y_3(x) = a\,(\log(b\,x))^{-1} + d\,.$$

The parameters obtained in the fitting are shown in Table 5. The curve $y_1(x)$ shows the biggest mean square error and mean absolute error o of the fitting. The relative uncertainties of curves $y_2(x)$ and $y_3(x)$ are quite similar, but the MSE and the MAE obtained by fitting to the curve $y_3(x)$ are several orders of magnitude smaller. Also, the best relative uncertainty obtained is not reached with the fitting, but it is achieve using the result of the finest mesh, the simulation with the highest number of mesh elements.

Using the relative deformation of the cavity over pressure obtained in Table 5 for $y_2(x)$ and the finest mesh, the values of Table 1 and the Equation (9) is possible to calculate the pressure that the Fabry-Perot cavity will have for a given nominal pressure. The difference between the calculated and nominal

Table 5. Values of the mean square error (MSE) of the fit, the mean absolute error (MAE) of the fit and κ in Pa^{-1} for each fit and the value of κ for the finest mesh.

$y_1(x) = a\,x^{-4} + b\,x^{-2} + c\,x^{-1} + d$		
MSE	MAE	
7.36×10^{-18}	1.97×10^{-9}	
κ	$u(\kappa)$	$u(\kappa)/\kappa$
$-5.758610 \times 10^{-12}$	1.9	3.3×10^{-6}
$y_2(x) = a\,x^{-2} + b\,x^{-1} + d$		
MSE	MAE	
9.17×10^{-30}	2.51×10^{-15}	
κ	$u(\kappa)$	$u(\kappa)/\kappa$
$-5.758573 \times 10^{-12}$	1.1×10^{-17}	1.9×10^{-6}
$y_3(x) = a\,(\log(b\,x))^{-1} + d$		
MSE	MAE	
3.19×10^{-34}	1.24×10^{-17}	
κ	$u(\kappa)$	$u(\kappa)/\kappa$
$-5.758600 \times 10^{-12}$	1.5×10^{-17}	2.6×10^{-6}
κ of the finest mesh (2602131elements)		
κ	$u(\kappa)$	$u(\kappa)/\kappa$
$-5.7585840x10^{-12}$	4.7×10^{-18}	8.2×10^{-7}

Table 6. Comparison between the results of the first model analysed by the partners (Model 1 partner) and analysed by CEM (Model 1 CEM) and the cylindrical model (Model 2).

Model	Pressure-normalized deformation (κ) $(\Delta L/L)/P$ in 10^{-12} Pa^{-1}	Uncertainty in 10^{-12} Pa^{-1}
Model 1 partner	-6.3902	0.00015
Model 1 CEM	-6.3842	0.032
Model 2	-5.758584	0.00000047

Figure 15. Relative difference between calculated pressure and nominal pressure $(P_{\text{Nominal}} - P)/P_{\text{Nominal}}$.

Figure 16. Relative uncertainty of calculated pressure with κ_1 and κ_2 versus the nominal pressure.

values are shown in Figure 15. The asymptotic behaviour is shown again, and the difference of the relative difference obtained with these values is so small that over pressures of 100 Pa cannot be distinguish (under 7×10^{-10}). The values of relative difference between the nominal pressure and the calculated values of pressure are similar to the obtained in Figure 6.

As it was discussed before the relative uncertainty of pressure depends on the nominal pressure (Equation (10) and (11)). Figure 16 represents the evolution of pressure uncertainty with the nominal pressure. A linear dependency is shown again and the increase of the uncertainty using the value obtained with the curve $y_2(x)$ is bigger than the obtained with the finest mesh. Furthermore, this simulation gives the best relative uncertainty, under 6.5×10^{-14} for both cases.

Table 6 shows a comparison between the best values of pressure-normalized deformation obtained for each model, including the results obtained by the partners. It is shown that the cylindrical model presents less pressure-normalized deformation and uncertainty.

7. FINAL DISCUSSION

The results of the simulations of the Fabry-Perot cavity deformation proposed by CNAM depends on the number of mesh elements introduced in the FEM software to simulate it. Also, different software can have different results. Because of this issue, a study of the evolution of the relative deformation over pressure of the Fabry-Perot cavity was made, fitting curve to two equations in order to achieve the value when the number of mesh elements tends to infinity obtaining a relative error in κ between 5×10^{-5} and 3×10^{-4} depending on the curve used.

Moreover, the propagation of uncertainty of κ to the pressure was studied for the values obtained with this method, showing that the formula which fits the best is $y_1(x) = \frac{a}{x^4} + \frac{b}{x^2} + \frac{c}{x} + d$ whose parameters are collected in Table 5. It was shown, that the relative difference with the nominal value of pressure is under 5×10^{-7} times the value of the nominal pressure and an asymptotic behaviour was shown in Figure 6.

Furthermore, the difference between values of pressure-normalized deformation obtained by other laboratories were compared with the values calculated using Solid Edge software. We conclude that the relative difference between the nominal pressure and the calculated pressure is under 5×10^{-8} times the value of the nominal pressure for 10 kPa. Also, the difference between the values obtained by the CEM and the pressure calculated using the κ of [1] is under 4×10^{-8} times the value of the pressure calculated with the κ of [1]. For Figure 8 and Figure 9, the asymptotic behaviour shown before was followed.

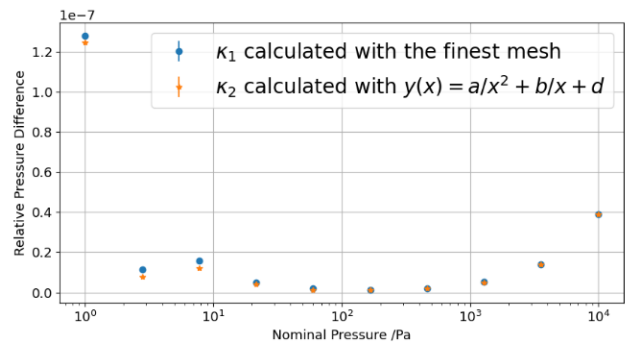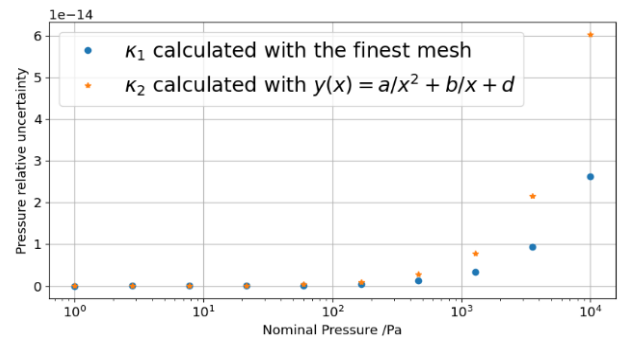Moreover, the pressure relative uncertainty calculated for both cases is under 3×10^{-10} times the nominal pressure, which means that the contribution of the uncertainty of pressure-normalized deformation (κ), for a range of pressure between 1 Pa and 10 kPa, to the relative pressure uncertainty is not decisive for the measure.

Finally, the CEM's Fabry-Perot cavity provides smaller pressure-normalized deformation (-5.7548684 $\times 10^{-12}$ Pa^{-1}) with an uncertainty of 4.7×10^{-18} Pa^{-1}, which is 0.1 times smaller than the other cavity. The Fabry-Pérot cylindrical cavity provides a relative uncertainty under 6.5×10^{-14} for 10 kPa, one order of magnitude less than the best results using the other geometry. It would be interesting making a study of the deformation of the mirrors for different Fabry-Pérot cavity configurations.

8. CONCLUSION

In conclusion, CEM's results using finite elements method through the software Solid Edge are similar to the results presented in [1] (with a discrepancy of 0.001 times the values obtained by [1]).

Also, the CEM's cylindrical has a pressure-normalized relative deformation 0.1 times lower than the model analysed in [1]. Moreover, the model presents more advantages as it only uses one material and, with the selected dimensions, there is a more laminar regimen in rapid pressure variations.

In future projects the uncertainties of the constants and values of Table 1 will be introduced in order to have a value of the total uncertainty of the measurement. Also, due to the capability of the cylindrical design to have an inner pressure different to the outer pressure, an analysis of the FP cavity deformation where vacuum is applied inside the cavity and atmospheric pressure is applied outside the cavity will be studied.

REFERENCES

[1] J. Zakrisson, I. Silander, C. Forssén, Z. Silvestri, D. Mari, S. Pasqualin, A. Kussicke, P. Asbahr, T. Rubin, O. Axner, Simulation of pressure-induced cavity deformation - the 18SIB04 Quantumpascal EMPIR project, ACTA IMEKO 9(5) (2020), pp. 281-286.
DOI: 10.21014/acta_imeko.v9i5.985

[2] I. Silander, T. Hausmaninger, M. Zelan, O. Axner, Gas modulation refractometry for high-precision assessment of pressure under non-temperature-stabilized conditions, Journal of Vacuum Science & Technology 36(3) (2018), art. 03E105, pp. 1-8.
DOI: 10.1116/1.5022244

[3] O. Axner, I. Silander, T. Hausmaninger, M. Zelan, Drift-free Fabry-Perot-cavity-based optical refractometry-Accurate expressions for assessments of gas refractivity and density, Jan. 2018.
DOI: 10.48550/ARXIV.1704.01187

[4] Pauli Virtanen (+ 34 authors), SciPy 1.0: Fundamental algorithms for scientific computing in Python, Nature Methods 17(3) (2020), pp. 261-272.
DOI: 10.1038/s41592-019-0686-2

[5] Z. Silvestri, F. Boineau, P. Otal, J. Wallerand, Helium-Based refractometry for pressure measurements in the range 1-100 kPa, in 2018 Conference on Precision Electromagnetic Measurements (CPEM 2018), July 08-13, 2018, Paris, France.
DOI: 10.1109/CPEM.2018.8501259